

pubs.acs.org/JCTC Article

Does the Traditional Band Picture Describe the Electronic Structure of Doped Conjugated Polymers? TD-DFT and Natural Transition Orbital Study of Doped P3HT

Eric C. Wu* and Benjamin J. Schwartz*



Cite This: J. Chem. Theory Comput. 2023, 19, 6761–6769



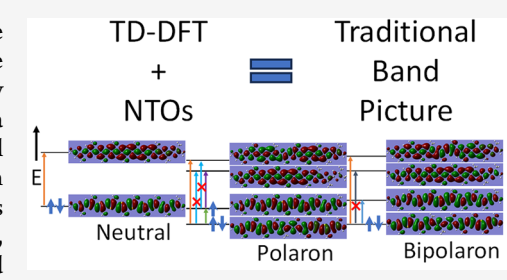
ACCESS I

Metrics & More

Article Recommendations

Supporting Information

ABSTRACT: Polarons and bipolarons are created when one or two electrons are removed from the π -system of a p-type conjugated polymer, respectively. In the traditional band picture, the creation of a polaron causes two electronic energy levels to move into the band gap. The removal of a second electron to form a bipolaron causes the two intragap states to move further into the gap. Several groups, however, who looked at the energies of the Kohn–Sham orbitals from DFT calculations, have recently argued that the traditional band picture is incorrect for explaining the spectroscopy of doped conjugated polymers. Instead, the DFT calculations suggest that polaron creation causes only one unoccupied state to move into the band gap near the valence band edge while half-filled state in



the valence band and the conduction band bend downward in energy. To understand the discrepancy, we performed TD-DFT calculations of polarons and bipolarons on poly(3-hexylthiophene) (P3HT). Not only do the TD-DFT-calculated absorption spectra match the experimental absorption spectra, but an analysis using natural transitional orbitals (NTOs), which provides an approximate one-electron picture from the many-electron TD-DFT results, supports the traditional band picture. Our TD-DFT/NTO analysis indicates that the traditional band picture also works for bipolarons, a system for which DFT calculations were unable to determine the electronic structure.

1. INTRODUCTION

Organic semiconducting conjugated polymers, such as poly(3-hexylthiophene-2,5-diyl) (P3HT; see Scheme 1a for chemical structure), have found applications in flexible electronic devices, such as light-emitting diodes, photovoltaics, and thermoelectric devices. ^{1–6} For these applications, conjugated polymer films are often oxidized (p-type doping) or reduced (n-type doping) to introduce equilibrium charge carriers on the π -conjugated polymer backbone.

For p-type conjugated polymers, such as P3HT, when an electron is removed from the π system, the backbone locally changes structure from aromatic to quinoidal, as depicted in Scheme 1b. The unpaired electron and positive charge that remain, along with the changes in the bonding structure, are together termed a polaron. If the oxidative driving force to remove electrons is strong enough, then polaronic P3HT can be oxidized a second time, removing the unpaired electron. This second oxidation removes the radical character on the polymer backbone, and the resulting spinless doubly charged species is referred to as a bipolaron, depicted in Scheme 1c. The question that we focus on in this work is how to think about the electronic structure and spectroscopy of polarons and bipolarons in doped conjugated polymers.

Most papers in the literature treat the charge carriers on doped conjugated polymers using the traditional band picture borrowed from the language of inorganic semiconductors.^{7–14}

In this picture, the distortion of the conjugated backbone caused by the aromatic-to-quinoid structural change causes two states associated with the unpaired electron to move into the band gap; one of these states is half-filled and the other is empty, as depicted in the center diagram of Scheme 1d. The presence of these two midgap electronic states creates two new optically allowed transitions, usually labeled P1 and P2, as well as two transitions that are optically forbidden by symmetry but may be weakly allowed in some cases, ¹⁵ usually labeled P3 and P3', as also shown in the center panel of Scheme 1d. For doped P3HT, the lower-energy P1 transition usually occurs in the mid-infrared with a peak between 0.3 and 0.6 eV, while the higher-energy P2 transition appears roughly an eV below the band gap, usually in the near-infrared around 1.4—1.5 eV.

For bipolarons, the traditional picture involves removing the unpaired electron from the lower intragap state. The addition of another positive charge causes the backbone structure to further distort, causing the two intragap states to move even further into the gap (i.e., away from the band edges), as shown in the right-

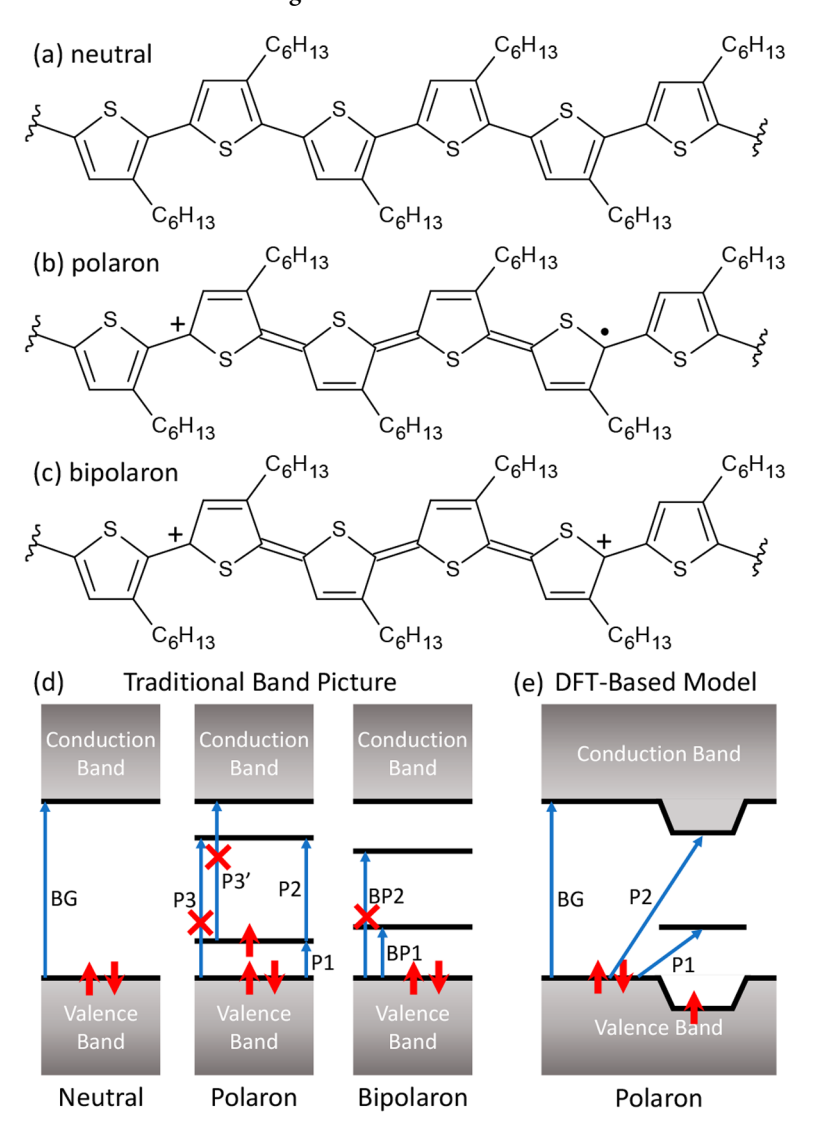
Received: July 5, 2023

Published: September 28, 2023





Scheme 1. Chemical Structures of (a) Neutral P3HT, (b) Polaronic P3HT, and (c) Bipolaronic P3HT; (d) the Energy Level Diagrams for Neutral P3HT, Polaronic P3HT, and Bipolaronic P3HT for the Traditional Band Picture (left, center, and right, respectively) and (e) the DFT-Based "Band-Bending" Model for Polarons^a



"BG is the band-gap transition. P1, P2, P3, and P3' are the optical transitions associated with polarons, while BP1 and BP2 are the transitions associated with bipolarons. The P3, P3', and BP2 optical transitions are nominally forbidden by symmetry.

most diagram of Scheme 1d.¹⁷ This leads to two transitions, an optically allowed transition labeled BP1 and a higher-energy optically forbidden transition labeled BP2. Although there has been some controversy regarding whether the BP1 transition is observed to the blue or the red of the P1 transition for doped P3HT, ^{18–20} previous work from our group ²¹ and other groups ^{22–24} has shown that the P3HT BP1 transition indeed appears to the blue of the P1 transition, typically occurring between 0.8 and 1.1 eV. Indeed, we recently argued that the new peaks that appear to the red of P1 at high doping concentrations should be assigned to coupled polarons and not to bipolarons.²¹

Despite the fact that basic observations of the P1, P2, and BP1 transitions seem to fit well with the traditional band picture, several groups have argued on the basis of quantum chemistry calculations that borrowing the traditional band picture of conjugated polymer doping from inorganic semiconductors is incorrect.^{25–31} These groups used density-functional theory (DFT)-based calculations, and upon examination of the density

of states of the Kohn–Sham orbitals yielded by such calculations, concluded that polaron creation causes only one unoccupied state to move into the band gap and that states in the conduction and valence bands associated with the unpaired electron bend downward in energy. Let a lie be low the top of the valence band instead of in the band gap as in the traditional band picture; we have previously referred to this view as the "band-bending picture". In the band-bending picture, exciting the P1 transition causes an electron to move from the valence band to an unoccupied state in the gap and exciting the P2 transition causes an electron to move from the valence band to the bent-down region of the conduction band. Several groups recently have used the band-bending picture to interpret experimental results.

One of the strongest criticisms of the traditional band picture is based on the ionization energies of neutral versus polaronic P3HT.²⁷ Cyclic voltammetry shows clearly that the ionization

energy of polaronic P3HT is roughly 300 meV higher than that of neutral P3HT, ²¹ a result that makes sense since second ionization energies are always higher than first ionization energies; this is because the second electron needs to be removed in the presence of an already-existing positive charge. In the traditional band picture, because the half-filled state is drawn as having moved up in energy from the valence band into the band gap, one could conclude that the electron in this state is easier to ionize (i.e., has a lower ionization energy) than the electrons that remain in the valence band, a result that would be unphysical. The band-bending picture remedies this apparent contradiction by putting the half-filled state below the top of the valence band, so that removal of the unpaired electron would indeed require a higher ionization energy.

On the other hand, the DFT-based band-bending picture has several short-comings. First, the band-bending picture does not account for the presence of P3 or P3' transitions, which are nominally forbidden by symmetry but sometimes experimentally observed. 15,36 Moreover, without explicitly included counterions, bipolarons are not bound in DFT calculations, ^{21,26,37,38} so there is no DFT-based "band-bending" picture of the electronic structure of bipolarons.²⁷ Lastly, a few years ago, our group attempted to test whether the traditional or the band-bending picture of doped conjugated polymer electronic structure makes more sense by performing ultrafast transient absorption spectroscopy experiments on polarons in doped P3HT.³² The resulting pattern of transient absorptions and bleaches seen in the experiments fit perfectly with what would be expected from the traditional band picture; the results were not consistent with the band bending picture, which predicts a different pattern of transient bleaches and absorptions. 27,32 In addition, we also performed ultrafast spectroscopy experiments exciting the BP1 transition of a different conjugated polymer doped to produce bipolarons, and again found results that were consistent with the traditional band picture.³⁹

All of this leads to the main questions addressed in this paper: which picture, traditional or DFT-based band-bending, better represents the electronic structure of doped conjugated polymers? Which picture gives a more accurate description of the transitions observed in spectroscopy? If the traditional picture is correct, how does one connect the multielectron character of the energy levels in high-level quantum chemistry calculations to simplified one-electron states used in diagrams like those in Scheme 1d? And is there a quantum-chemistry-based explanation for the ionization energy ordering of neutral and doped conjugated polymers?

Here, we address these questions through a series of timedependent DFT (TD-DFT) calculations combined with an analysis based on natural transition orbitals (NTOs). TD-DFT, by construction, generates a multielectron description of the transitions between the occupied and unoccupied energy levels, but we show that NTO analysis applied to such calculations allows us to construct a qualitatively accurate one-electron picture of the transitions involved. We find that unlike standard DFT calculations, which predict the band-bending picture based on energy levels inferred from Kohn-Sham orbitals, the physically meaningful excited states generated by TD-DFT calculations and the orbitals generated from NTO analysis yield the traditional picture for the P1 and P2 transitions of doped conjugated polymers. We also find that the TD-DFT-calculated difference in ionization energies of neutral and doped P3HT are in reasonable agreement with experiment: the calculations suggest that the presence of the positive charge associated with the polaron shifts the vacuum level so that the absolute energy level of the polaronic half-filled state is lower than that of the valence band for the neutral polymer, similar to the bandbending picture. Taken together with previous experiments, our TD-DFT calculations strongly suggest that the traditional band picture, although not perfect, is the best way to think about the electronic structure and optical transitions of doped conjugated polymers.

2. RESULTS AND DISCUSSION

To answer the questions posed above, TD-DFT and NTO calculations were done on hydrogen-terminated P3HT oligomers with 10 monomers using the Gaussian 09 package. 40 We chose this oligomer length because our previous theoretical work showed that this was sufficient to properly describe polarons on doped P3HT;²¹ use of oligomers of this length is also consistent with recent experiments by Stanfield et al., 41 who demonstrated that polarons in doped P3HT have a spatial extent of ~5 to 7 repeat units, depending on the P3HT crystallinity. To further reduce the computational cost, we replaced the P3HT hexyl side chains in our calculations by methyl groups. All systems were geometry-optimized using DFT calculations with the 6-31G(d,p) basis set and the PBE0 functional in the presence of a polarizable continuum model (PCM) with $\epsilon = 3$, chosen to match the experimentally measured dielectric constant of P3HT. 42 Although long-range corrected functionals often perform better in many systems, we found that the structure of oxidized P3HT optimized with ω PBE puts the polaron at one end of the oligomer rather than in the middle, a situation that we did not feel was realistic, as shown in Figure S3 of the Supporting Information (SI). We also found that the TD-DFT-calculated ω PBE absorption spectrum was significantly different from that observed experimentally, as shown in Figure S4 in the SI. Thus, for this work, we focus on calculations with the geometry optimization performed with the PBE0 functional because it gives a more realistic picture of both polarons and bipolarons than the long-range corrected ωPBE functional.

We then performed TD-DFT calculations on the optimized structures using the same basis set and functional. We also performed TD-DFT calculations using the long-range corrected ω PBE functional, both with the range-separation parameter, ω , set to the default value, 0.4 bohr⁻¹, and with ω set to 0.1882 bohr⁻¹, the value used by Heimel et al. to develop the bandbending picture. A detailed discussion comparing the results obtained with the different functionals is included in the SI, but regardless of the functionals chosen, the one-electron orbitals generated from NTO analysis are qualitatively similar and support the traditional band picture's description of the P1 and P2 transitions. For the discussion below, we focus on the results obtained with the PBE0 functional, which provides a TD-DFT-calculated spectrum that best agrees with experiment.

For polaronic P3HT, a single point-charge counterion was placed at a distance of 7.5 Å from the center of the chain in the direction along the side chains, matching the experimentally documented position of the anions in F_4TCNQ -doped P3HT films. For bipolaronic P3HT, point-charge counterions were placed on opposite sides of the center of the chain at a distance of 5 Å, as required for bipolarons to be bound in this system. For geometry optimization with point charge(s), the terminal hydrogen atoms at the ends of the chain and one carbon atom at the middle of the chain (one of the carbon atoms that bridges monomer 5 and monomer 6) are fixed during geometry optimization. By fixing the positions of these three atoms, all the

bonds are still able to fully relax, which was checked via frequency calculations.

Although the use of point charges to represent the counterions may seem overly simplistic, previous work 41,43,45,46 has shown that point charges provide an adequate description of the Coulomb interaction between (bi)polarons and their counterions. For example, Spano and co-workers 43,46 showed that the use of point charges perfectly captures the experimentally seen shifts in the P1 peak position based on the polaron-anion distance. Moreover, our previous study on bipolarons²¹ used a point-charge model and was able to successfully assign the spectroscopic signatures of bipolarons and coupled polarons in doped conjugated polymers. The atomic positions for the optimized geometries are listed in the SI and the optimized geometries, including the counterion positions, are shown in Figure S1. For bipolaronic P3HT, our calculations were performed with multiplicity = 1 and only the closed-shell state was considered. The precise chain and counterion geometries are the same as those explored in our previous work.²¹

To benchmark our use of TD-DFT as a quantum chemistry method to determine the electronic structure of doped conjugated polymers, in Figure 1 we compare the calculated and experimental absorption spectra of neutral and (bi)polaronic P3HT. As expected for any DFT-based method, 47 the calculated spectra are slightly blue-shifted from experiment, but remarkably, the two sets of spectra are quite similar. The TD-DFT-calculated neutral P3HT spectrum has its band gap transition at 2.06 eV, only slightly blue of the experimental spectrum whose band gap transition is near 1.9 eV. For the TD-DFT-calculated P3HT polaron, the P1 and P2 transitions are seen around 0.63 and 1.45 eV, respectively, again only slightly blue of those seen experimentally. For P3HT bipolarons, the BP1 transition appears around 0.8 eV in experiments and 0.95 eV in our TD-DFT calculations. The fact that the calculated and experimental spectra agree so well for neutral, polaronic, and bipolaronic P3HT strongly suggests that the TD-DFT calculations are producing reasonable energy gaps to the excited states when determining the energies of these transitions.

One potential difference between the experimental and calculated spectra is that in addition to the experimentally expected P1, P2, and BG transitions, the TD-DFT calculations also show several other transitions that are weakly allowed. We will discuss this issue in more detail further below, but our NTO analysis shows that some of these are weakly allowed mixtures of the P1 and P2 transitions.

Given that TD-DFT does an excellent job reproducing the experimental spectroscopy, the next question is what is the underlying electronic structure? This is not a straightforward question to answer, however, because the transitions calculated from TD-DFT are described as a superposition of multiple individual transitions between Kohn-Sham orbitals, reflecting the multielectron character of such calculations. For example, Table 1 lists the 11 most important Kohn-Sham orbital transitions that comprise the 1.45 eV "P2" absorption transition in the calculated spectrum of the P3HT polaron (the transition marked with an asterisk in Figure 1b). Given that the eigenenergies of individual Kohn-Sham orbitals are not physically meaningful, this superposition makes it quite difficult to visualize the relevant multielectron energy levels underlying the calculated absorption spectrum.

To remedy this situation and restore an approximate oneelectron picture to the observed transitions to the extent

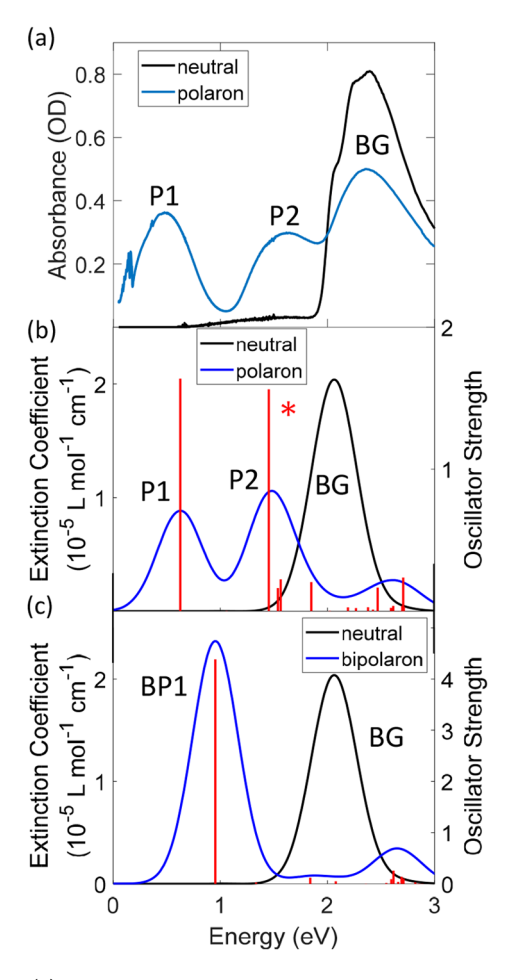


Figure 1. (a) Experimental absorption spectra of pristine P3HT (black curve) and FeCl3-doped P3HT films (blue curve). (b) PBE0/6-31G(p,d) TD-DFT calculated transition oscillator strengths (red sticks) and absorption spectra (calculated by assuming each individual transition has a Gaussian band shape with a fwhm of 0.6 eV) for a neutral P3HT 10-mer (black curve) and a polaron on a P3HT 10-mer (blue curve); panel c shows the same for a bipolaron on a P3HT 10mer. For the experimental spectra, the P3HT films were cast from a 20 mg mL⁻¹ solution of P3HT in o-dichlorobenzene. The doped film was created using sequential processing with a 1 mM solution of FeCl₃ in nbutylacetate. The transition marked with an asterisk in panel b is the 1.45 eV "P2" transition listed in Table 1 whose NTOs are shown in Figure 2.

Table 1. TD-DFT Description of the 1.45 eV "P2" Transition^a of the P3HT Polaron

Transitions ^b	Weights	Transitions ^b	Weights
$249A \rightarrow 252A$	0.16527	$248B \rightarrow 251B$	-0.20172
$249A \rightarrow 254A$	0.13536	$249B \rightarrow 254B$	0.10962
$250A \rightarrow 252A$	-0.10327	$250B \rightarrow 251B$	0.14560
$251A \rightarrow 253A$	-0.27689	$250B \rightarrow 252B$	0.21509
$251A \rightarrow 252A$	0.78010	$250B \rightarrow 253B$	0.22477
$251A \rightarrow 253A$	0.15173		

^aThis is the transition that is marked with an asterisk in Figure 1b. ^bOrbital 250 is the HOMO and 251 is the SOMO; A and B indicate the spin of the corresponding electron.

possible, we have examined the natural transition orbitals (NTOs) associated with our calculated TD-DFT spectra, which was not performed in previous works. 25–27 NTO analysis works by applying unitary transformations to the occupied and virtual

orbitals, so that each optical transition is compactly assigned as occurring mainly between a single occupied and a single unoccupied orbital. For example, when we apply NTO analysis to the P3HT polaron 1.45 eV P2 transition whose Kohn—Sham makeup is described in Table 1, we find that this absorption feature can be well-represented by a single transition between the two orbitals shown in Figure 2, with an NTO

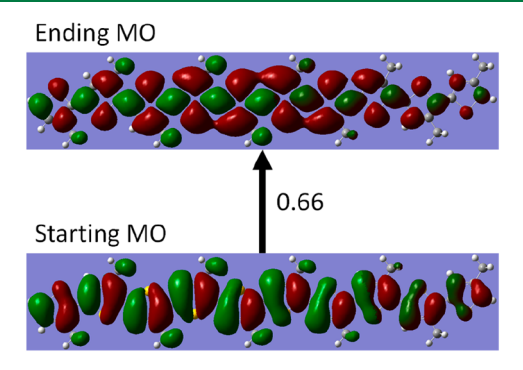


Figure 2. Starting and ending MO's for the 1.45 eV P2 transition of the P3HT polaron (the starred transition in Figure 1b whose Kohn—Sham composition is given in Table 1) generated using NTO analysis of our PBE0/6-31G(p,d) TD-DFT calculations on a P3HT 10-mer. The natural transition orbital coefficient between these two orbitals is 0.66, which means that this particular absorption feature is 66% accounted for by a one-electron transition between these two orbitals. A similar analysis for the other polaronic and bipolaronic transitions of P3HT is given in the SI.

weight of 0.66. In other words, for the heavily mixed 1.45 eV P2 polaron absorption, the two orbitals shown in Figure 2 account for 66% of the observed transition, so that this absorption feature can be fairly well approximated by the transition of a single electron between these two orbitals.

In addition to simplifying the visualization of the transitions underlying the TD-DFT calculated absorption spectrum, NTOs also provide a way to construct the underlying one-electron energy level diagram. For example, for the P3HT polaron, NTO analysis shows us directly that the ending orbital of the 0.63 eV P1 transition is the same as the starting orbital of the 1.45 eV P2

transition, as documented in more detail in the SI. Since we know the transition energies between these orbitals, this tells us that the energy gap between the starting orbital of the 0.63 eV transition and the ending orbital of the 1.45 eV transition must be roughly 2.03 eV. Thus, by examining the starting and ending NTOs of all of the TD-DFT calculated transitions, we can qualitatively construct TD-DFT-based one-electron energy level diagrams of neutral, polaronic, and bipolaronic P3HT. The one-electron energy-level diagram for P3HT extracted from our NTO analysis on our TD-DFT calculations is summarized in Figure 3.

The left part of Figure 3 shows the energy level diagram for neutral P3HT, whose calculated absorption spectrum has a single peak at 2.06 eV. The NTO analysis of this transition shows a starting one-electron orbital with aromatic thiophene rings spread over the entire P3HT 10-mer and an ending one-electron orbital with quinoidal thiophene rings. This fits with our chemical intuition that the P3HT band gap transition is a π -to- π^* transition.

The central portion of Figure 3 shows the NTOs and underlying energy level diagram for the P3HT polaron. The starting one-electron orbital of the 0.63 eV P1 transition has a central quinoidal thiophene ring sandwiched between aromatic thiophene rings, which fits well with the expected Lewis structure of the polaron shown in Scheme 1b. The ending orbital of this transition has aromatic thiophene rings throughout the chain. Moreover, as mentioned above, the starting orbital of the 1.45 eV P2 transition also has aromatic thiophene rings throughout the P3HT 10-mer, indicating that the ending orbital of the P1 transition is the starting orbital for the P2 transitions. It is worth remembering, however, that the single-electron transitions between the pair of NTOs pictured in Figure 3 are only approximations of the true TD-DFT transitions. However, for the purpose of creating the most accurate simple singleelectron picture that explains the spectroscopy of doped semiconducting polymers, we believe that it is reasonable to assign the various optical transitions as occurring between the NTOs pictured in Figure 3.

In contrast with the one-electron picture developed with our NTO analysis, in the one-electron band-bending picture, the P1 and P2 transitions should have the same one-electron starting

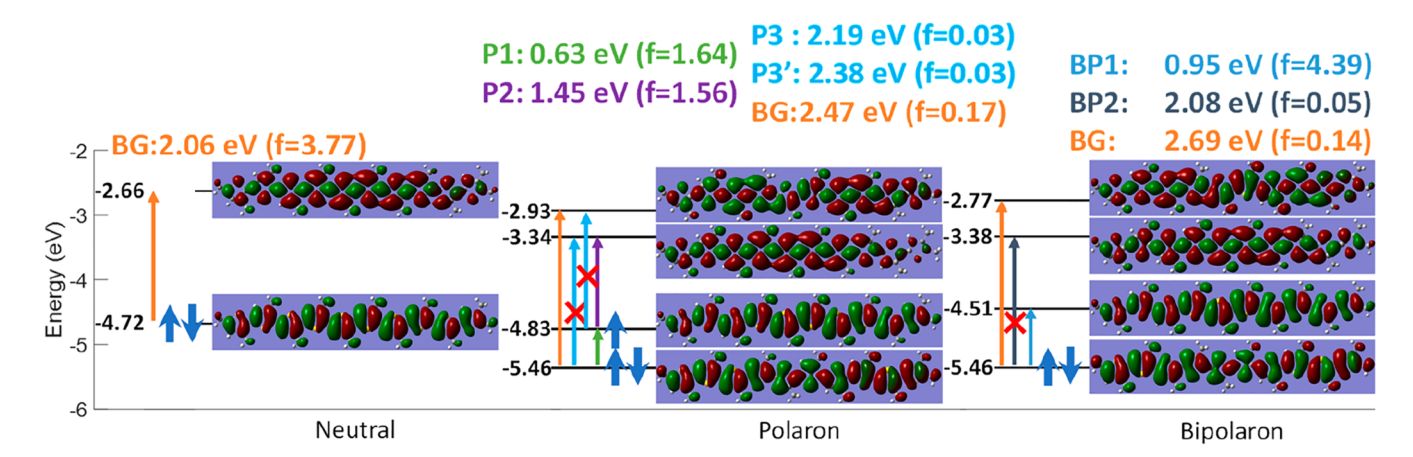


Figure 3. Absolute one-electron energy levels and corresponding NTOs from PBE0/6-31G(p,d) TD-DFT calculations for a neutral (left), a polaronic (center), and a bipolaronic (right) P3HT 10-mer. The energy levels of each species clearly resemble those of the traditional band picture and not the DFT-based band-bending picture shown in Scheme 1. Note that the presence of the positive charge associated with the polaron shifts the vacuum level (or correspondingly lowers all of the occupied energy levels) so that the ionization energy of the polaron SOMO is larger than that of the neutral. In other words, the traditional band picture works well as long as the vacuum level shift is properly accounted for.

orbital, whereas the traditional band picture predicts that the ending orbital for the P1 transition is the starting orbital for the P2 transition. Therefore, our NTO analysis of the P3HT polaronic absorption transitions indicates that electronic structure and the optical transitions obtained via TD-DFT is much more like the traditional band picture than the bandbending picture; our analysis is also in better agreement with the pattern of bleaches and transient absorptions seen in pump/ probe experiments on doped conjugated polymers. ^{32,39}

As mentioned above, in addition to the P1 and P2 transitions, our TD-DFT calculations show a few additional weakly allowed transitions, such as the ones at 1.54 and 1.56 eV in Figure 1b. The one-electron NTOs associated with these transitions can be found in the SI, and the analysis shows that these are mixtures of P1 and P2 transitions. For example, the 1.54 eV transition can be described as having 30% P1 transition and 21% P2 transition character, and the 1.56 eV transition has 56% P1 transition and 25% P2 transition character. For constructing a simplified one-electron energy level diagram, however, we believe it makes sense not to include these transitions since their oscillator strengths are much lower than the P1 and P2 transitions, and thus they would not be visible under the strongly allowed bands seen experimentally.

In the traditional band picture, the P3 transition, which is usually forbidden by symmetry, should be from the HOMO to the LUMO, which means it should have the same starting oneelectron orbital as the 0.63 eV P1 transition and the same ending orbital as the 1.45 eV P2 transition. Based on this picture, the TD-DFT-predicted transition at 2.19 eV, which has a small oscillator strength of ~0.03, is the P3 transition. Indeed, the NTO analysis shows that the starting orbital of the 2.19 eV transition has a central quinoidal thiophene ring between aromatic thiophene rings, clearly the same as the starting orbital of the 0.63 eV P1 transition. The ending orbital of the 2.19 eV transition has quinoidal thiophene rings throughout the chain, matching the ending orbital of the 1.45 eV P2 transitions. And of course, the low oscillator strength of the 2.19 eV transition agrees with the traditional band picture in which the P3 transition is symmetry forbidden.¹⁵

We also note that NTO analysis also shows that the 2.38 eV P3' transition has the same starting orbital of the 1.45 eV P2 transition and an ending orbital that is the same ending orbital of the 2.47 eV BG transition. As mentioned above, there is no P3 or P3' transition, forbidden or otherwise, predicted in the bandbending picture, but the TD-DFT calculations, which support the traditional picture via NTO analysis, are able to predict the 2.19 eV P3 and 2.38 eV P3' transitions in the calculated spectrum. Finally, our NTO analysis shows that the 2.47 eV transition for the P3HT polaron, which corresponds to the remaining BG absorption, clearly has the same starting orbital as the 0.63 eV P1 transition, which again is consistent with the traditional picture and experiment.

Overall, the one-electron energy level scheme obtained when combining all the multielectron TD-DFT-calculated transitions with NTO analysis (Figure 3) looks remarkably like the traditional band picture shown in Scheme 1d. We note that there are some subtle differences between the traditional band picture and the TD-DFT-based energy levels. For example, the traditional picture predicts that the BG transition energy should be roughly the P2 transition energy plus twice the P1 transition energy; it also predicts that the forbidden P3 transition energy should roughly equal the sum of the P1 and P2 transition energies. Our TD-DFT calculations indeed suggest that the BG

transition energy is roughly equal to twice the P1 plus the P2 transition energies but the TD-DFT P3 and P3' transition energies are somewhat larger than the sum of the P2 and P1 transition energies. This could be because of the particular functional and basis set used for the TD-DFT calculations, or it could be a reflection of the fact that the traditional band picture is overly simplified in that it does not account for the multielectron mixed nature of the underlying transitions. The important point, however, is that by combining TD-DFT calculations with NTO analysis, we are able to show that the one-electron energy levels and optical transitions of the P3HT polaron much better resemble the traditional band picture than the band-bending picture based on standard DFT.

We can do a similar TD-DFT-based NTO analysis for the energy levels of the P3HT bipolaron, which is summarized in the right portion of Figure 3. As mentioned above, a bipolaron forms when the unpaired electron is removed from the SOMO of the P3HT polaron. In the traditional band picture, this should cause the two intragap states to move further into the gap, leaving three transitions, BP1, BP2, and the BG, that should all share the same one-electron starting orbital. Our TD-DFT-based NTO analysis of bipolaronic P3HT shows that indeed, the calculated 0.95, 2.08, and 2.69 eV transitions share the same starting orbital, consistent with their assignments as the BP1, BP2, and BG transitions, respectively. We also see that the starting NTO for these three transitions is similar to that of the P1 transition for the P3HT polaron other than the bipolaron NTO shows two central quinoidal thiophene rings instead of only one for the polaron. This observation fits well with our previous work, which showed that bipolarons have a similar structure to polarons but with a larger quinoidal distortion of the P3HT backbone.²¹ And, as the traditional band picture suggests, the two intragap states move further into the gap, explaining why the BP1 transition at 0.95 eV lies to the blue of the P1 transition at 0.63 eV.7-9 As mentioned above, there is no corresponding band-bending picture based on DFT for the bipolaron, so the fact that our calculations match well with experiment indicates that they are successfully capturing the underlying electronic structure.²

With TD-DFT-based energy level diagrams established for neutral, polaronic, and bipolaronic P3HT that all match well with the traditional band picture, we close by examining the relative energies between the different P3HT ionization states. Our TD-DFT calculations place the HOMO energy levels for neutral and polaronic P3HT at -4.72 and -5.46 eV relative to vacuum, respectively. We note that the experimental position of the neutral P3HT HOMO is usually taken to be ~ -5.0 eV, $^{51-53}$ so that the TD-DFT calculations are off by several hundred meV, which is not all that surprising given the importance of electron correlation in conjugated polymers with delocalized π MOs that is treated only approximately by DFT.

Even though the absolute TD-DFT energy levels are somewhat off, Bellafont et al. have argued that shifts in electron binding energies can be accurately obtained from DFT-based energy levels. Given this and the relative ordering of the energy levels seen in Figure 3, this would put the SOMO level of the polaron P3HT at -4.83 eV relative to vacuum. This positioning suggests that polaronic P3HT is ~ 100 meV harder to oxidize than the neutral P3HT, which is somewhat less than the ~ 300 meV that is seen experimentally. The difference between the calculated value and experimental value is most likely due to our choice of positioning of the counterions in the calculation (Table S1 shows how the anion distance affects the difference between the first and second ionization energies); it could also

be due to the choice of functional or finite chain length. Another possibility is that since bipolaron formation requires loss of polymer crystallinity, ^{21,55} the experimentally measured difference in ionization energy includes the energy needed to disrupt the P3HT crystal structure, something that is not included in the present calculations that only examine electronic effects.

Whatever the case, TD-DFT correctly predicts that the ionization energy of neutral P3HT is less than that of a positively charged P3HT polaron. We believe that the confusion in the literature was based on the fact that when the traditional band pictures for neutral and polaronic P3HT are drawn side-by-side, as in Scheme 1d, it appears that the polaron SOMO lies above the neutral P3HT HOMO. However, the presence of the positive charge shifts the vacuum level (or correspondingly lowers all of the P3HT energy levels because the remaining electrons are all attracted to the net positive charge), so that on an absolute scale, the polaron is harder to oxidize than the neutral polymer (and the bipolaron is harder to oxidize than the polaron), as expected. When the shift of the vacuum level is accounted for (by aligning the energy levels using TD-DFT calculated excited states and NTO analysis), the traditional band picture works quite well.

3. CONCLUSIONS

In summary, the work presented here shows that when using DFT-based quantum chemistry calculations to describe the electronic structure and the optical transitions of doped conjugated polymers, two important things must be taken into account. First, although it is computationally more expensive, TD-DFT is necessary to obtain meaningful excited states to correctly determine the differences between the occupied and unoccupied multielectron energy levels associated with P3HT polarons and bipolarons. This is because the use of traditional DFT, where the calculated energy gaps between one-electron states involve unoccupied Kohn-Sham orbitals whose energies have no physical meaning, gives results that are not consistent with experiment. Second, it is important to use NTO analysis to correctly identify which effective one-electron energy levels have the same character for neutral P3HT and the P3HT polaron and bipolaron to properly align the location of the occupied valence band levels for the different charged P3HT species.

Overall, despite some controversy in the literature over the best way to think about the electronic structure and optical transitions of polarons on doped conjugated polymers, our TD-DFT calculations and NTO analysis suggest that the traditional band picture works well for explaining the spectroscopy of the different charged states of P3HT. The traditional band picture also can explain the relative ionization energies of the different charged states of P3HT as long as one accounts for the shift of the vacuum level in the presence of the polaronic charge(s). We note that after accounting for the vacuum level shift, the energy levels of the occupied and half-filled states in the traditional picture look very similar to those in the band-bending picture. However, the assignments of the P1 and P2 transitions in the band-bending picture, ^{25–27} which are based on the Kohn-Sham orbital energies from DFT calculations, are inconsistent with both the TD-DFT calculations presented here and with ultrafast spectroscopy experiments that have measured the pattern of bleaches and excited-state absorptions of photoexcited polarons on P3HT. 32,39 Our TD-DFT/NTO picture also suggests that the traditional band picture also holds for bipolarons, a system that could not be properly described by the DFT-based bandbending picture. Thus, even though the underlying details of the

TD-DFT electronic structure are complex, when combined with NTO analysis, they support the idea the traditional band picture of doped conjugated polymers works quite well as a simplified explanation for understanding the behavior of these interesting materials.

ASSOCIATED CONTENT

Supporting Information

The Supporting Information is available free of charge at https://pubs.acs.org/doi/10.1021/acs.jctc.3c00743.

A discussion on how counterion geometries affect relative ionization energy, a discussion on the starting orbital of the BG transition of the neutral P3HT vs the ending orbital of the P1 transition of the polaronic P3HT, a discussion on the energy of the VB level of the polaronic P3HT vs bipolaronic P3HT, atomic positions for neutral, polaronic, and bipolaronic P3HT, a discussion on calculations using hydrogen-terminated vs methyl-terminated P3HT oligomers, a discussion on the use of TD-DFT calculations with different functionals, and descriptions of the TD-DFT transitions and the corresponding NTOs for neutral, polaronic, and bipolaronic P3HT (PDF)

AUTHOR INFORMATION

Corresponding Authors

Eric C. Wu – Department of Chemistry and Biochemistry, University of California, Los Angeles, Los Angeles, California 90095-1569, United States; Email: wueric@ucla.edu

Benjamin J. Schwartz — Department of Chemistry and Biochemistry, University of California, Los Angeles, Los Angeles, California 90095-1569, United States; o orcid.org/0000-0003-3257-9152; Email: schwartz@chem.ucla.edu

Complete contact information is available at: https://pubs.acs.org/10.1021/acs.jctc.3c00743

Notes

The authors declare no competing financial interest.

ACKNOWLEDGMENTS

We gratefully acknowledge the support of funding from the National Science Foundation through grant number NSF DMR-2105896. Computations were performed on the Hoffman 2 cluster operated by the UCLA Institute for Digital Research and Education.

REFERENCES

- (1) Dou, L.; You, J.; Hong, Z.; Xu, Z.; Li, G.; Street, R. A.; Yang, Y. 25th Anniversary Article: A Decade of Organic/Polymeric Photovoltaic Research. *Adv. Mater.* **2013**, 25 (46), 6642–6671.
- (2) Kuik, M.; Wetzelaer, G.-J. A. H.; Nicolai, H. T.; Craciun, N. I.; De Leeuw, D. M.; Blom, P. W. M. 25th Anniversary Article: Charge Transport and Recombination in Polymer Light-Emitting Diodes. *Adv. Mater.* **2014**, 26 (4), 512–531.
- (3) Russ, B.; Glaudell, A.; Urban, J. J.; Chabinyc, M. L.; Segalman, R. A. Organic Thermoelectric Materials for Energy Harvesting and Temperature Control. *Nature Reviews Materials* **2016**, *1* (10), 16050.
- (4) Cowart, J. S.; Liman, C.; Garnica, A.; Page, Z. A.; Lim, E.; Zope, R. R.; Baruah, T.; Hawker, C. J.; Chabinyc, M. L. Donor-Fullerene Dyads for Energy Cascade Organic Solar Cells. *Inorg. Chim. Acta* **2017**, 468, 192–202.
- (5) Hou, L.; Zhang, X.; Cotella, G. F.; Carnicella, G.; Herder, M.; Schmidt, B. M.; Pätzel, M.; Hecht, S.; Cacialli, F.; Samorì, P. Optically

- Switchable Organic Light-Emitting Transistors. *Nat. Nanotechnol.* **2019**, *14* (4), 347–353.
- (6) Kaloni, T. P.; Giesbrecht, P. K.; Schreckenbach, G.; Freund, M. S. Polythiophene: From Fundamental Perspectives to Applications. *Chem. Mater.* **2017**, *29* (24), 10248–10283.
- (7) Bredas, J. L.; Street, G. B. Polarons, Bipolarons, and Solitons in Conducting Polymers. *Acc. Chem. Res.* **1985**, *18* (10), 309–315.
- (8) Nowak, M.; Rughooputh, S. D. D. V.; Hotta, S.; Heeger, A. J. Polarons and Bipolarons on a Conducting Polymer in Solution. *Macromolecules* **1987**, *20* (5), 965–968.
- (9) Beljonne, D.; Cornil, J.; Sirringhaus, H.; Brown, P. J.; Shkunov, M.; Friend, R. H.; Brédas, J.-L. Optical Signature of Delocalized Polarons in Conjugated Polymers. *Adv. Funct. Mater.* **2001**, *11* (3), 229–234.
- (10) Bubnova, O.; Khan, Z. U.; Wang, H.; Braun, S.; Evans, D. R.; Fabretto, M.; Hojati-Talemi, P.; Dagnelund, D.; Arlin, J.-B.; Geerts, Y. H.; Desbief, S.; Breiby, D. W.; Andreasen, J. W.; Lazzaroni, R.; Chen, W. M.; Zozoulenko, I.; Fahlman, M.; Murphy, P. J.; Berggren, M.; Crispin, X. Semi-Metallic Polymers. *Nat. Mater.* **2014**, *13* (2), 190–194.
- (11) Fichou, D.; Horowitz, G.; Xu, B.; Garnier, F. Stoichiometric Control of the Successive Generation of the Radical Cation and Dication of Extended α -Conjugated Oligothiophenes: A Quantitative Model for Doped Polythiophene. *Synth. Met.* **1990**, *39* (2), 243–259.
- (12) Kahmann, S.; Loi, M. A.; Brabec, C. J. Delocalisation Softens Polaron Electronic Transitions and Vibrational Modes in Conjugated Polymers. *J. Mater. Chem. C* **2018**, *6* (22), 6008–6013.
- (13) Campbell, D. K.; Bishop, A. R.; Fesser, K. Polarons in Quasi-One-Dimensional Systems. *Phys. Rev. B* **1982**, 26 (12), 6862–6874.
- (14) Chung, T.-C.; Kaufman, J. H.; Heeger, A. J.; Wudl, F. Charge Storage in Doped Poly(Thiophene): Optical and Electrochemical Studies. *Phys. Rev. B* **1984**, *30* (2), 702–710.
- (15) Wang, C.; Duong, D. T.; Vandewal, K.; Rivnay, J.; Salleo, A. Optical Measurement of Doping Efficiency in Poly(3-Hexylthiophene) Solutions and Thin Films. *Phys. Rev. B* **2015**, *91* (8), 085205.
- (16) Fuzell, J.; Jacobs, I. E.; Ackling, S.; Harrelson, T. F.; Huang, D. M.; Larsen, D.; Moulé, A. J. Optical Dedoping Mechanism for P3HT:F4TCNQ Mixtures. *J. Phys. Chem. Lett.* **2016**, 7 (21), 4297–4303.
- (17) Colaneri, N.; Nowak, M.; Spiegel, D.; Hotta, S.; Heeger, A. J. Bipolarons in Poly(3-Methylthiophene): Spectroscopic, Magnetic, and Electrochemical Measurements. *Phys. Rev. B* **1987**, *36* (15), 7964–7968.
- (18) Qarai, M. B.; Ghosh, R.; Spano, F. C. Understanding Bipolarons in Conjugated Polymers Using a Multiparticle Holstein Approach. *J. Phys. Chem. C* **2021**, 125 (44), 24487–24497.
- (19) Enengl, C.; Enengl, S.; Pluczyk, S.; Havlicek, M.; Lapkowski, M.; Neugebauer, H.; Ehrenfreund, E. Doping-Induced Absorption Bands in P3HT: Polarons and Bipolarons. *ChemPhysChem* **2016**, *17* (23), 3836–3844.
- (20) Balooch Qarai, M.; Ghosh, R.; Hestand, N. J.; Spano, F. C. Multipolaron Complexes in Conducting Polymers: The Importance of Hole-Hole Repulsion in Charge Delocalization. *J. Phys. Chem. C* **2023**, 127 (13), 6414–6424.
- (21) Wu, E. C.; Salamat, C. Z.; Ruiz, O. L.; Qu, T.; Kim, A.; Tolbert, S. H.; Schwartz, B. J. Counterion Control and the Spectral Signatures of Polarons, Coupled Polarons, and Bipolarons in Doped P3HT Films. *Adv. Funct Materials* **2023**, 33, 2213652.
- (22) Salem, N.; Lavrisa, M.; Abu-Lebdeh, Y. Ionically-Functionalized Poly(Thiophene) Conductive Polymers as Binders for Silicon and Graphite Anodes for Li-Ion Batteries. *Energy Technology* **2016**, *4* (2), 331–340.
- (23) Thomas, E. M.; Davidson, E. C.; Katsumata, R.; Segalman, R. A.; Chabinyc, M. L. Branched Side Chains Govern Counterion Position and Doping Mechanism in Conjugated Polythiophenes. *ACS Macro Lett.* **2018**, *7* (12), 1492–1497.
- (24) Gordon, M. P.; Gregory, S. A.; Wooding, J. P.; Ye, S.; Su, G. M.; Seferos, D. S.; Losego, M. D.; Urban, J. J.; Yee, S. K.; Menon, A. K. Microstructure and Heteroatom Dictate the Doping Mechanism and Thermoelectric Properties of Poly(Alkyl-Chalcogenophenes). *Appl. Phys. Lett.* **2021**, *118* (23), 233301.

- (25) Zozoulenko, I.; Singh, A.; Singh, S. K.; Gueskine, V.; Crispin, X.; Berggren, M. Polarons, Bipolarons, And Absorption Spectroscopy of PEDOT. ACS Applied Polymer Materials 2019, 1 (1), 83–94.
- (26) Sahalianov, I.; Hynynen, J.; Barlow, S.; Marder, S. R.; Müller, C.; Zozoulenko, I. UV-to-IR Absorption of Molecularly p-Doped Polythiophenes with Alkyl and Oligoether Side Chains: Experiment and Interpretation Based on Density Functional Theory. *J. Phys. Chem. B* **2020**, *124* (49), 11280–11293.
- (27) Heimel, G. The Optical Signature of Charges in Conjugated Polymers. ACS Central Science 2016, 2 (5), 309–315.
- (28) Winkler, S.; Amsalem, P.; Frisch, J.; Oehzelt, M.; Heimel, G.; Koch, N. Probing the Energy Levels in Hole-Doped Molecular Semiconductors. *Mater. Horiz.* **2015**, *2* (4), 427–433.
- (29) Png, R.-Q.; Ang, M. C. Y.; Teo, M.-H.; Choo, K.-K.; Tang, C. G.; Belaineh, D.; Chua, L.-L.; Ho, P. K. H. Madelung and Hubbard Interactions in Polaron Band Model of Doped Organic Semiconductors. *Nat. Commun.* **2016**, *7* (1), 11948.
- (30) Kohlstedt, K. Mind the Gap. ACS Central Science 2016, 2 (5), 278-280.
- (31) Kahmann, S.; Fazzi, D.; Matt, G. J.; Thiel, W.; Loi, M. A.; Brabec, C. J. Polarons in Narrow Band Gap Polymers Probed over the Entire Infrared Range: A Joint Experimental and Theoretical Investigation. *J. Phys. Chem. Lett.* **2016**, *7* (22), 4438–4444.
- (32) Voss, M. G.; Scholes, D. T.; Challa, J. R.; Schwartz, B. J. Ultrafast Transient Absorption Spectroscopy of Doped P3HT Films: Distinguishing Free and Trapped Polarons. *Faraday Discuss.* **2019**, *216*, 339–362.
- (33) Umar, A. R.; Dorris, A. L.; Kotadiya, N. M.; Giebink, N. C.; Collier, G. S.; Grieco, C. Probing Polaron Environment in a Doped Polymer via the Photoinduced Stark Effect. *J. Phys. Chem. C* **2023**, *127* (20), 9498–9508.
- (34) Lungwitz, D.; Joy, S.; Mansour, A. E.; Opitz, A.; Karunasena, C.; Li, H.; Panjwani, N. A.; Moudgil, K.; Tang, K.; Behrends, J.; Barlow, S.; Marder, S. R.; Brédas, J.-L.; Graham, K.; Koch, N.; Kahn, A. Spectral Signatures of a Negative Polaron in a Doped Polymer Semiconductor: Energy Levels and Hubbard *U* Interactions. *J. Phys. Chem. Lett.* **2023**, *14* (24), 5633–5640.
- (35) Tsokkou, D.; Peterhans, L.; Cao, D. X.; Mai, C.; Bazan, G. C.; Nguyen, T.; Banerji, N. Excited State Dynamics of a Self-Doped Conjugated Polyelectrolyte. *Adv. Funct. Mater.* **2020**, *30* (9), 1906148.
- (36) Aubry, T. J.; Axtell, J. C.; Basile, V. M.; Winchell, K. J.; Lindemuth, J. R.; Porter, T. M.; Liu, J.; Alexandrova, A. N.; Kubiak, C. P.; Tolbert, S. H.; Spokoyny, A. M.; Schwartz, B. J. Dodecaborane-Based Dopants Designed to Shield Anion Electrostatics Lead to Increased Carrier Mobility in a Doped Conjugated Polymer. *Adv. Mater.* **2019**, *31* (11), 1805647.
- (37) Zamoshchik, N.; Bendikov, M. Doped Conductive Polymers: Modeling of Polythiophene with Explicitly Used Counterions. *Adv. Funct. Mater.* **2008**, *18* (21), 3377–3385.
- (38) Zamoshchik, N.; Salzner, U.; Bendikov, M. Nature of Charge Carriers in Long Doped Oligothiophenes: The Effect of Counterions. *J. Phys. Chem. C* **2008**, *112* (22), 8408–8418.
- (39) Voss, M. G.; Challa, J. R.; Scholes, D. T.; Yee, P. Y.; Wu, E. C.; Liu, X.; Park, S. J.; León Ruiz, O.; Subramaniyan, S.; Chen, M.; Jenekhe, S. A.; Wang, X.; Tolbert, S. H.; Schwartz, B. J. Driving Force and Optical Signatures of Bipolaron Formation in Chemically Doped Conjugated Polymers. *Adv. Mater.* **2021**, *33* (3), 2000228.
- (40) Frisch, M. J.; Trucks, G. W.; Schlegel, H. B.; Scuseria, G. E.; Robb, M. A.; Cheeseman, J. R.; Scalmani, G.; Barone, V.; Petersson, G. A.; Nakatsuji, H.; Li, X.; et al. *Gaussian 09, Revision A.02*; Gaussian Inc: Wallingford, CT, 2016.
- (41) Stanfield, D. A.; Mehmedović, Z.; Schwartz, B. J. Vibrational Stark Effect Mapping of Polaron Delocalization in Chemically Doped Conjugated Polymers. *Chem. Mater.* **2021**, *33* (21), 8489–8500.
- (42) Wang, C.; Zhang, Z.; Pejić, S.; Li, R.; Fukuto, M.; Zhu, L.; Sauvé, G. High Dielectric Constant Semiconducting Poly(3-Alkylthiophene)s from Side Chain Modification with Polar Sulfinyl and Sulfonyl Groups. *Macromolecules* **2018**, *51* (22), 9368–9381.

- (43) Scholes, D. T.; Yee, P. Y.; Lindemuth, J. R.; Kang, H.; Onorato, J.; Ghosh, R.; Luscombe, C. K.; Spano, F. C.; Tolbert, S. H.; Schwartz, B. J. The Effects of Crystallinity on Charge Transport and the Structure of Sequentially Processed F 4 TCNQ-Doped Conjugated Polymer Films. *Adv. Funct. Mater.* **2017**, *27* (44), 1702654.
- (44) Stanfield, D. A.; Wu, Y.; Tolbert, S. H.; Schwartz, B. J. Controlling the Formation of Charge Transfer Complexes in Chemically Doped Semiconducting Polymers. *Chem. Mater.* **2021**, 33 (7), 2343–2356.
- (45) Wu, E. C.-K.; Salamat, C. Z.; Tolbert, S. H.; Schwartz, B. J. Molecular Dynamics Study of the Thermodynamics of Integer Charge Transfer vs Charge-Transfer Complex Formation in Doped Conjugated Polymers. ACS Appl. Mater. Interfaces 2022, 14 (23), 26988–27001.
- (46) Ghosh, R.; Chew, A. R.; Onorato, J.; Pakhnyuk, V.; Luscombe, C. K.; Salleo, A.; Spano, F. C. Spectral Signatures and Spatial Coherence of Bound and Unbound Polarons in P3HT Films: Theory Versus Experiment. *J. Phys. Chem. C* **2018**, *122* (31), 18048–18060.
- (47) Shao, Y.; Mei, Y.; Sundholm, D.; Kaila, V. R. I. Benchmarking the Performance of Time-Dependent Density Functional Theory Methods on Biochromophores. J. Chem. Theory Comput. 2020, 16 (1), 587–600.
- (48) Narsaria, A. K.; Ruijter, J. D.; Hamlin, T. A.; Ehlers, A. W.; Guerra, C. F.; Lammertsma, K.; Bickelhaupt, F. M. Performance of TDDFT Vertical Excitation Energies of Core-Substituted Naphthalene Diimides. J. Comput. Chem. 2020, 41 (15), 1448–1455.
- (49) Conradie, J.; Wamser, C. C.; Ghosh, A. Understanding Hyperporphyrin Spectra: TDDFT Calculations on Diprotonated Tetrakis(*p* -Aminophenyl)Porphyrin. *J. Phys. Chem. A* **2021**, *125* (46), 9953–9961.
- (50) Martin, R. L. Natural Transition Orbitals. J. Chem. Phys. 2003, 118 (11), 4775–4777.
- (51) Gao, W.; Kahn, A. Controlled p -Doping of Zinc Phthalocyanine by Coevaporation with Tetrafluorotetracyanoquinodimethane: A Direct and Inverse Photoemission Study. *Appl. Phys. Lett.* **2001**, 79 (24), 4040–4042.
- (52) Kivala, M.; Boudon, C.; Gisselbrecht, J.-P.; Enko, B.; Seiler, P.; Müller, I. B.; Langer, N.; Jarowski, P. D.; Gescheidt, G.; Diederich, F. Organic Super-Acceptors with Efficient Intramolecular Charge-Transfer Interactions by [2 + 2] Cycloadditions of TCNE, TCNQ, and F 4-TCNQ to Donor-Substituted Cyanoalkynes. *Chem. Eur. J.* **2009**, *15* (16), 4111–4123.
- (53) Jacobs, I. E.; Moulé, A. J. Controlling Molecular Doping in Organic Semiconductors. *Adv. Mater.* **2017**, 29 (42), 1703063.
- (54) Pueyo Bellafont, N.; Illas, F.; Bagus, P. S. Validation of Koopmans' Theorem for Density Functional Theory Binding Energies. *Phys. Chem. Chem. Phys.* **2015**, *17* (6), 4015–4019.
- (55) Banerji, N.; Tsokkou, D.; Cavassin, P.; Rebetez, G.; Bardagot, O. Terahertz Conductivity and Charge Transfer Dynamics in Electrochemically Doped P3HT. In *Advances in Ultrafast Condensed Phase Physics III*; Yakovlev, V., Haacke, S., Eds.; SPIE: Strasbourg, France, 2022; p 19. DOI: 10.1117/12.2628014.